



PLLA/nHA Composite Films and Scaffolds for Medical Implants: In Vitro Degradation, Thermal and Mechanical Properties

Esperanza Díaz^{1,2} · Ane Libe Molpeceres¹ · Iban Sandonis³ · Igor Puerto¹

Received: 3 August 2018 / Accepted: 11 September 2018 / Published online: 17 September 2018
© Springer Science+Business Media, LLC, part of Springer Nature 2018

Abstract

Two poly(L-lactide) (PLLA) materials and changes in their mechanical, thermal, physical, and chemical properties while undergoing in vitro degradation are studied. The potential applications of PLLA implants extend to films for controlled drug release systems and biodegradable scaffolds for bone implants (fabricated with thermal induced phase separation) (TIPS) using bioactive nanohydroxyapatite particles. The study was conducted in a phosphate buffer saline (PBS) solution at 37 °C over 8 weeks. Reinforcement with nHA particles increased the elastic modulus and the yield stress, due perhaps to restricted C–C bond rotations and polymer sliding, although that increase was not proportional with the added percentages of nanoparticles. The elastic modulus and the yield stress of the films decreased faster than those of the scaffolds. As from the seventh week some samples could not be tested due to the fragility of the specimens. The scaffolds had a higher enthalpy of fusion than the films, suggesting that crystalline domains formed more easily in the scaffolds than in the films. The films degraded more quickly than the scaffolds, because the acid products resulting from the degradation process were evacuated from the films with greater difficulty than from the scaffolds in which the autocatalytic effect was of greater importance. Porosity was decisive in the rate of degradation.

Keywords Films · Scaffolds · In vitro degradation · Thermal properties · Mechanical properties

1 Introduction

Medical grade polymers used in medical implants may be classified by their durability as either long term stable or biodegradable materials in accordance with their functional life. Permanent polymers include all implants of a permanent nature, such as systems or devices used in either total or partial substitution of tissue and organs destroyed as a consequence of illness or traumatic injury. In either context,

both polymethyl methacrylate (PMMA) and polyethylene (PE) may be mentioned [1, 2].

Degradable polymeric biomaterials must be biocompatible with tissues and can degrade over a certain time following their implantation giving rise to products that are not toxic and that will be either eliminated or metabolized by the body such as polylactide (PLA) or polycaprolactone (PCL). Both are hydrolytically degradable, PCL being a rather long lasting polymer. Drug delivery systems and tissue engineering matrices may be highlighted among the temporal applications within the organism [3, 4].

The controlled drug delivery and release systems permit the body to make better use of the medication, because the action of the drug is prolonged over time, which in turn is an advantage for the patient that consumes them. The designed absorption speed of polymeric matrix in this application is important for the administration of the medication at the correct dosage and at the right time. Polymeric waste is rapidly metabolized by the body [5–7].

In the case of the biodegradable polymers used in tissue engineering, they should have mechanical properties that are capable of supporting the application until the

✉ Esperanza Díaz
esperanza.diaz@ehu.es

¹ Escuela de Ingeniería de Bilbao, Departamento de Ingeniería Minera, Metalúrgica y Ciencia de Materiales, Universidad del País Vasco (UPV/EHU), C/María Díaz de Haro, nº 68, 48920 Portugalete, Spain

² BCMaterials, Edif. Martina Casiano, Pl.3 Parque Científico UPV/EHU, Barrio Sarriena s/n, 48940 Leioa, Spain

³ Escuela de Ingeniería de Bilbao, Departamento de Física Aplicada I, Universidad del País Vasco (UPV/EHU), 48920 Portugalete, Spain

tissue has scarred, without provoking any inflammatory or toxic process. They should be metabolized by the body after complying with their function, be easily processed, be easy to sterilize and their durability should be acceptable [3, 4, 8].

There are several factors that influence the inflammatory response of the body with respect to the polymer, such as chemical composition, porosity, roughness of the surface, implant morphology, degradation rate, and products resulting from the degradation process [8, 9].

The hydrolytic degradation of aliphatic polyesters [10–13] might be due to surface degradation mechanisms or en-bloc degradation. If the hydrolytic rupture of the chains and consequent production and diffusion of oligomers and monomers into the environment is quicker than the entry of water into the polymer, then surface degradation will occur. Hence, the polymer will be reduced throughout the degradation process from the exterior towards the interior, with no effect on its interior, meaning that its molecular weight is maintained. The advantage of this quite predictable type of degradation can be very useful in applications such as drug delivery systems that control the speed of release.

En-bloc degradation occurs when the water penetrates inside the polymeric matrix, causing hydrolysis reactions within it and reducing the molecular weight of the set. In addition, if diffusion is sufficient, the resulting oligomers and monomers will spread in a uniform way throughout the matrix and all of the polymer will be equally degraded. In contrast, if the diffusion is hindered, the acidic products of the degradation process that react with the ester group chains at the end of the bonds will accumulate in the inside; giving rise to a self-catalyzed degradation reaction, degrading the interior more quickly than the exterior, where the diffusion of these products will be easier and the reduction of molecular weight will be slower [11–13].

Many authors have studied the degradation of films and scaffolds [9, 14, 15], however, there are relatively few results on the effects of nanoparticles such as nanohydroxyapatite.

Hence, we conducted a comparison between two poly-L-lactide (PLLA) medical implants in this study contrasting thermal and mechanical properties and the in-vitro degradation of films that can be used as drug delivery and controlled release systems and biodegradable scaffolds for bone implants (fabricated with thermal induced phase separation) (TIPS) using bioactive nanohydroxyapatite particles. With this purpose in mind, we analyzed the changes in mechanical and thermal properties, water uptake, pH, the sample weight, morphology, and molecular weight. Although some conclusions drawn from the in vitro study of these systems are not extrapolable to the in vivo conditions, in vitro degradation offers very valuable information on the behavior of that material in vivo.

2 Experimental

2.1 Materials

Optically pure poly-L-lactide (PLLA) containing less than 0.01% of residual solvent and less than 0.1% residual monomer was supplied by Biomer L9000 (Germany). The solvent, chloroform (Panreac p.a. Barcelona, Spain), was distilled by conventional methods. The weight-average relative molecular weight $M_w = 142,000$, $M_n = 95,700$ and polydispersity $M_w/M_n = 1.5$ of PLLA were determined using gel permeation chromatography (GPC, Perkin Elmer 200) in tetrahydrofuran (THF). GPC was performed with a THF solvent using a Perkin Elmer 200 reflective index detector. Calibration was done in accordance with polystyrene standards with a flow rate of 1 ml/min. Phosphate buffer solution in water (PBS), supplied by Fluka Analytical (Sigma Aldrich, USA) at a pH of 7.2, was used as the degradation fluid.

2.2 Fabrication of Films and Porous Scaffolds

PLLA and PLLA/nHA composite films and scaffolds were synthesized according to a protocol. In brief, the PLLA was dissolved in chloroform [2.5% (w/v)]. Then, nHA particles were homogeneously dispersed in the above suspension by ultrasonic stirring. Films and highly porous composite scaffolds with different nHA proportions of total polymer mass (0%, 10%, 30%, 50%) were obtained after evaporation for the films and after freezing and freeze-drying (TIPS) the resultant solutions for several days for the scaffolds. Porous foam scaffolds with porosities of up to 75–89% were obtained by this method [16, 17].

2.3 In Vitro Degradation

In preparation for the degradation experiment, the samples were finely cut into 11 mm by 2 mm disks, weighed, and totally immersed in glass test tubes, filled with 10 ml of PBS, where they were evenly incubated in a thermostated oven at 37 °C. The specimens were recovered after 2, 4, 6, and 8 weeks under the same conditions, carefully wiped and then weighed to determine water absorption [18, 19]. A pH meter PCE 228 by PCE Instruments (Spain) was used to determine the pH alteration in the medium. Eventually, the degraded samples were dried over 2 additional weeks to a constant weight.

Water absorption and mass loss were evaluated by weighing, taking into account the original weight of each sample (W_0) and the residual weight, after degradation of the same specimen (W_r) that had completely dried. The water

absorption percentage, $W_a\%$, was calculated by the following equation:

$$W_a\% = (W_w - W_r)/W_r \times 100 \quad (1)$$

where W_w is the weight of the wet specimen after the removing surface water.

Weight loss percentage ($W_L\%$) was estimated by the following equation:

$$W_L\% = (W_0 - W_r)/W_0 \times 100 \quad (2)$$

2.4 SEM Analysis

The bulk morphology of the scaffolds was examined using scanning electron microscopy (SEM) (HITACHI S-4800, Tokyo, Japan). Prior to analysis, the samples were coated with a layer of gold, in a JEL Ion Sputter JFC-1100 (Amiron Machinery, Oxnard, California) at 1200 V and 5 mA., to avoid sample charging under the electron beam.

2.5 DSC Analysis

DSC measurements were performed with a TA Instruments calorimeter. The samples were heated from -90 to 120 °C at 10 °C/min (1st run), then cooled at 10 °C/min, and finally heated at 10 °C/min (3rd run).

2.6 Mechanical Property

Mechanical testing of the pore scaffolds was performed using a Universal Testing Machine (Instron, Model: 4502UK). Fabrication of the films and porous scaffold has been described above. The disk diameter of the scaffold and films was 11 mm and disk thickness was 2 mm. The compressive modulus was defined as the initial linear modulus and the yield stress was determined from the intersection of the two tangents on the stress–strain curve around the yield point. Five films and scaffolds were mechanically tested for each sample.

3 Results and Discussion

3.1 Mechanical Properties

In previous works [16, 17] we have described a great variety of scaffolds, fabricated using TIPS, in which pore wall morphology and structure can be controlled by the previously mentioned phase separation parameters. When chloroform was used as solvent the scaffolds had a porosity of 75 – 89% . The compressive modulus and yield stress (see Fig. 1a, b respectively) increased with the added percentage of nanoparticles. The values of the mechanical properties of the scaffolds with a larger quantity of nHA

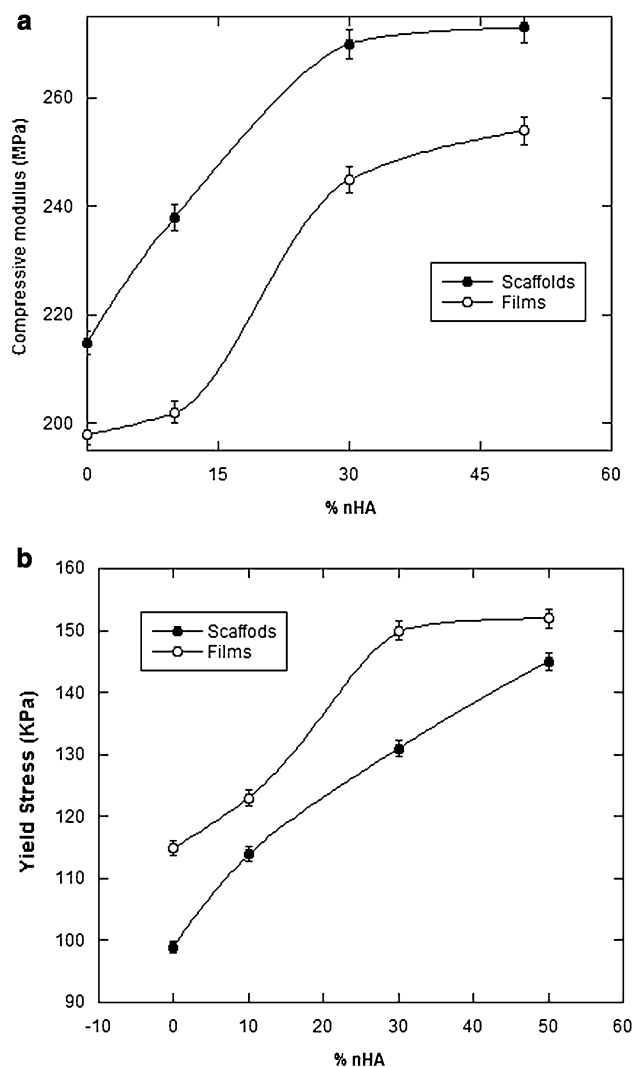


Fig. 1 **a** Compressive modulus of scaffolds and films versus of nHA (wt%). **b** Yield stress of scaffolds and films as a function of nHA (wt%)

(50 wt%) were not as high as expected, which was due to the tendency of the nanoparticles to agglomerate (50 wt%) and to distribute themselves in irregular ways throughout the scaffold. Agglomeration formed bigger particles with smaller surface areas, which led to a pronounced reduction in mechanical properties [18–20]. In previous works [11, 12] we have observed that the influence of the nHA particles is important, despite their nanometric scale and uniform distribution but the mechanical properties were not only dependent on the presence of nHA, but were also due to its high concentrations that decreased the pore size. The compressive modulus and the yield stress are heavily dependent on pore size. The lower mechanical properties of the scaffolds with larger pore sizes, which has also been observed by other authors, could be consistent with the reduced polymer content [21–23].

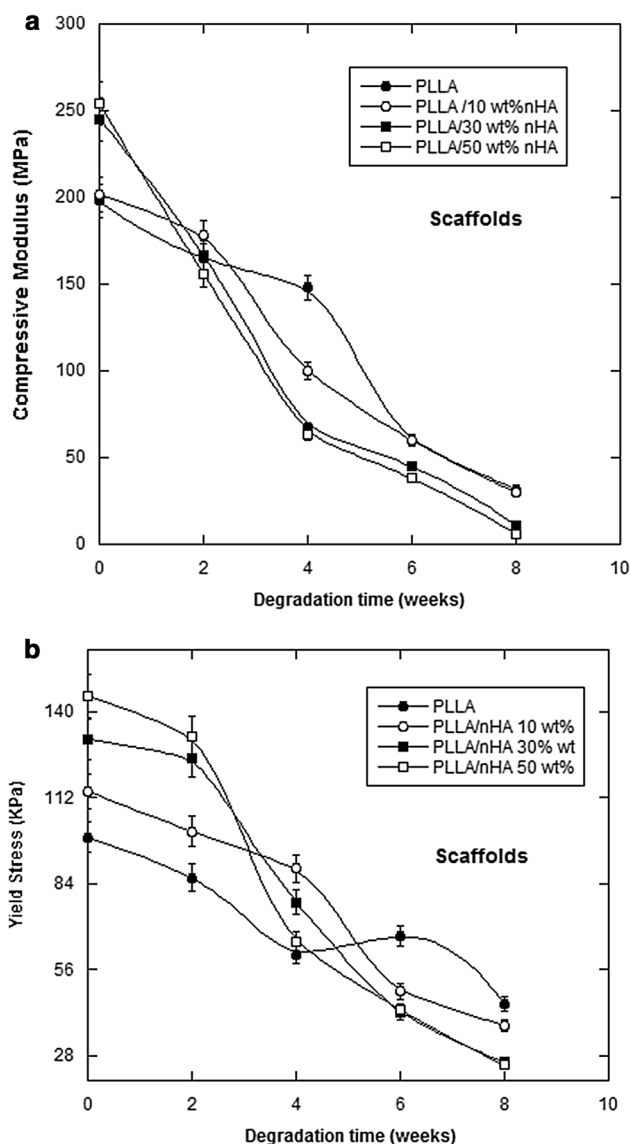


Fig. 2 a Compressive modulus of scaffolds as a function of degradation time (weeks). b Yield stress of scaffolds versus degradation time (weeks)

The mechanical properties of the scaffolds (compressive modulus and yield stress as a function of degradation time) can be seen in Fig. 2a, b. The pure PLLA scaffolds retained their mechanical properties over time, while the mechanical properties of the scaffolds fabricated with nHA decreased continuously as from week 4, during the degradation time, in such a way that the samples with a higher nHA wt% had after 8 weeks reached very low values. The values of compressive modulus and yield strength that were reached at the end of the degradation process were less than those obtained for the pure polymer [24, 25].

The compressive modulus and the yield stress values for the films (see Fig. 3a, b respectively) were higher than

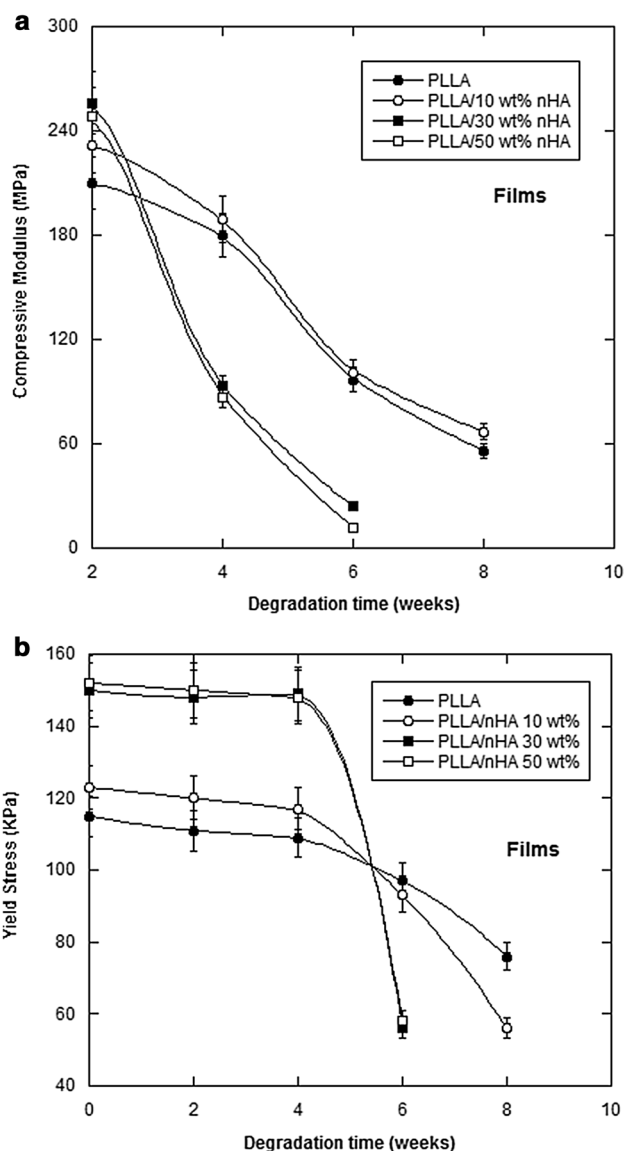


Fig. 3 a Compressive modulus of films as a function of degradation time (weeks). b Yield stress of films versus degradation time (weeks)

those of the scaffolds and their values remained relatively constant until the third week of degradation, after which they decreased very rapidly over time. Mechanical tests could not be performed on some samples as from week 7, due to the fragility of the test specimens. The experimental results showed that reinforcing with nHA particles increased the elastic modulus of PLLA/nHA and the yield stress, although as with the scaffolds, the increases were not proportional to the percentage of nHA. It may be argued that nHA particles, restricted C–C bond rotations, and polymer sliding all significantly increased the elastic modulus of the polymers. Also the crystallinity can contribute in this increase [24, 25].

3.2 Thermal Properties

The DSC peaks of the samples were analyzed to obtain the melting temperature, T_m , and the enthalpy of melting measured in the 1st run, ΔH_m , of the samples, for determination of the degree of crystallinity. The degree of crystallinity of the semicrystalline samples, X_C %, was obtained [26] from Eq. (3), where the enthalpy of melting of a 100% crystalline PLLA, $\Delta H_{m100\%}$, was reportedly 93 Jg^{-1} [27] and the enthalpy of melting of a semicrystalline sample was ΔH_m .

$$X_C(\%) = 100(\Delta H_m/\Delta H_{m100\%}) \quad (3)$$

T_g , T_m , and T_c remained practically invariable both for the scaffolds and for the films, at approximate values of 57, 170, and 115 °C, respectively.

In Fig. 4, we can see that the heat of melting (ΔH_m) increases for all film samples under study with the exception of the PLLA/ 10 wt% nHA system. The values of ΔH_m indicate an increase of crystallinity, for all samples studied, during the in vitro degradation. Some authors found that these values have to be carefully considered, because recrystallization may be induced during the heating [8, 28]. Other authors suggested that the increase was due to a rearrangement of the shortest chains generated by the specific degradation process with the consequent formation of new crystals. Some authors [29–31] explained this process by the hydrolysis of the ester bands that occur primarily in the amorphous regions, where the water penetrates more easily than in the highly arranged and densely packed crystalline regions, producing a hydrolytic degradation of the

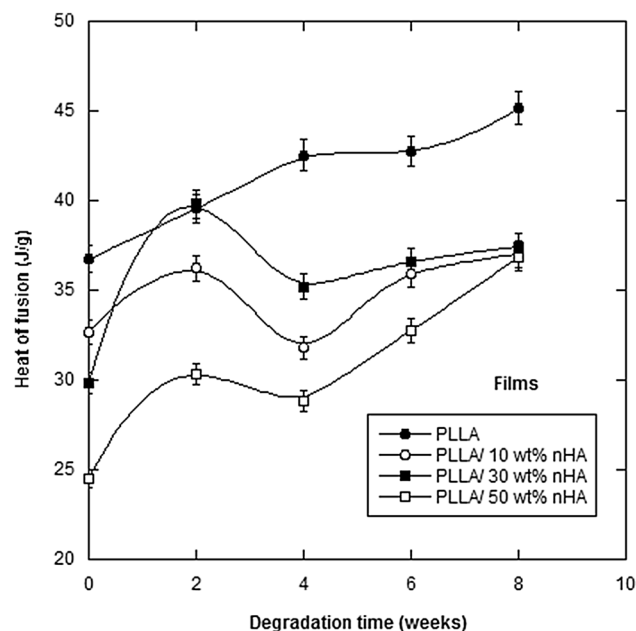


Fig. 4 Heat of fusion (Jg^{-1}) of films as a function of degradation time (weeks)

amorphous regions and a reorganization of both ends of the chain. A second phase began when the majority of the amorphous regions had degraded and the water had penetrated the crystalline regions. If we were in this phase, crystallinity would diminish as the crystalline parts would be affected. In our case, the incorporation of large amounts of nHA can form agglomerations that appear to act as a focal point for degradation processes (a behavior that has also been observed by SEM). In addition, the diffusion process is worse, as no pores exist, and the degradation products improve the autocatalytic degradation process.

We can see from Table 1 that the percentage of crystallinity increases at the end of the degradation process, regardless of the percentages of added nanoparticles. It is well known that higher crystallinity has a strong influence on the mechanical properties of a polymer, such as Young's modulus, yield stress, strain hardening rates, and ultimate tensile properties [32].

We found almost no variation in the enthalpy of fusion, $\Delta H_m = 42.5 \text{ (Jg}^{-1}\text{)}$, in our study of the scaffolds over 8 weeks of degradation, hence the degree of crystallinity remained practically invariable. This situation is because the PLLA scaffolds have hardly undergone degradation over that period of time. The enthalpy of fusion of the scaffolds is higher than that of the films $\Delta H_m \approx 30 \text{ (Jg}^{-1}\text{)}$, which may indicate that crystalline domains are formed more easily in scaffolds than in films; behaviors unlike those reported by other authors [8].

3.3 Water Absorption

Water absorption is the first effect that occurred when our films and scaffolds entered into contact with the aqueous medium (PBS) and it is a reflection of hydrolytic degradation. PLLA is hydrophobic and has semicrystalline structure that does allow fast water penetration into the PLLA bulk, the degradation kinetics were relatively rapid than other degradable polyester such as PCL [33]. In Fig. 5a, b, we can see the percentage water absorption as a function of the in vitro degradation time for the PLLA/nHA

Table 1 Percentage of crystallinity for films against degradation time (weeks)

Degradation time (weeks)	X_C % PLLA	X_C % PLLA/10 wt% nHA	X_C % PLLA/30 wt% nHA	X_C % PLLA/50 wt% nHA
0	0.87	4.24	1.63	2.94
2	8.69	10.44	9.26	2.58
4	9.85	7.34	3.42	2.44
6	8.23	5.01	3.38	7.26
8	11.77	9.14	5.03	12.63

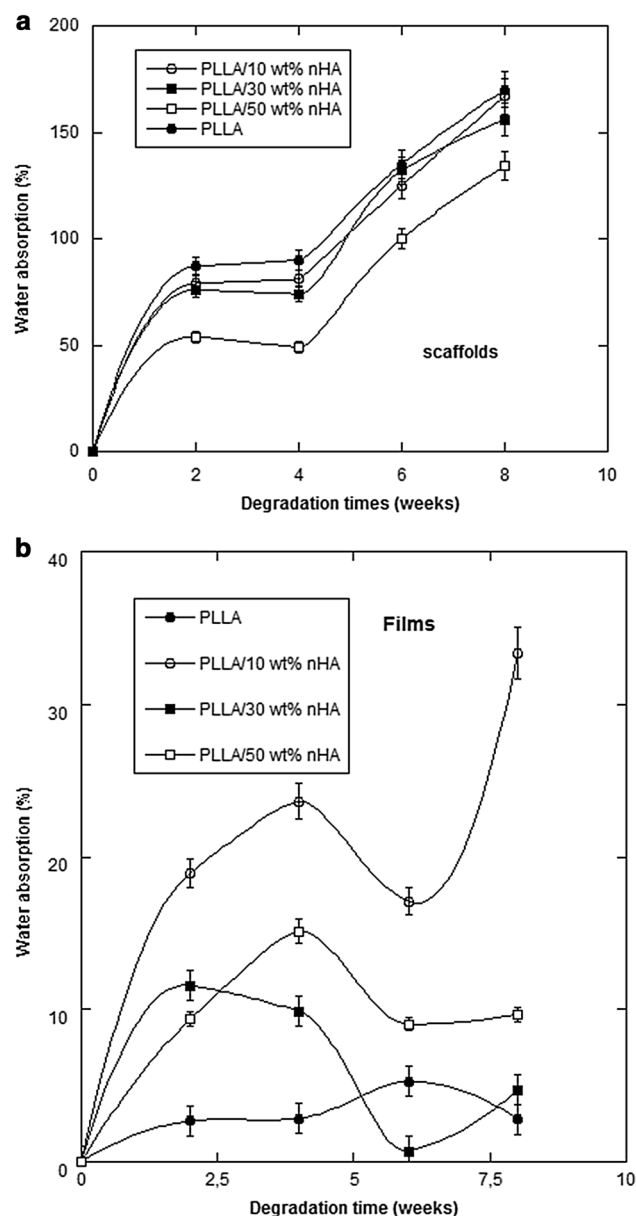


Fig. 5 **a** Water absorption of scaffolds as a function of degradation time (weeks). **b** Water absorption of films as a function of degradation time (weeks)

scaffolds and films. We can appreciate a very different behavior in both figures:

The general tendency of the scaffolds is to increase absorption up until the eighth week of degradation, reaching values of 170% with the PLLA sample without nHA. Three clearly different stages of degradation can be seen over the 8 weeks of *in vitro* degradation: a first stage up until week 2 during which there was a very significant uptake of water, a second stage up until week 4 in which a tendency towards stabilization may be seen, and a third stage corresponding to the weeks between the fourth and

the eighth week in which the absorption of PBS was very significant.

The higher the percentage of nanoparticles added to the samples, the higher the water absorption levels, with the exception of the film with 10 wt% of nHA, being the sample that absorbed most PBS. Two stages may be observed: one that lasted until week four of degradation in which sustained absorption of PBS may be observed, which was higher than 15% for the films with 10 and 50% nHA in comparison with 3 and 10% for the films with 0 and 30% nHA, respectively. The presence of larger amounts of nanoparticles increased the percentage absorption of PBS. As from the fourth week, there was a stabilization of water absorption for all the films under study. In other words [11, 12], when the absorption reached a specific value, its speed was reduced, as a result of the dissolution of the degradation products. These products introduced nHA particles inside the film, which slowed down the speed of degradation, due to the formation of alkaline solutions that acted as a physical barrier.

The films absorb very much less water than the scaffolds, even though the materials and therefore the hydrophilic nature of both is the same, because the higher porosity of the films means that they logically absorb more water more rapidly than the scaffolds. In addition, the amount of water absorbed is related to porosity and the amount of liquid water available on the surface of the material. Hence, the porous materials can uptake and store more water, while the non-porous or denser materials can store a limited amount of water. The incorporation of nHA increased the water uptake of both the compound scaffolds and the films. However, the films degraded much earlier, as we shall see later on [33, 34]. This water absorption process is a balance between the dissolution of oligomers in solution and the consumption of waste in the PBS. An increase in water absorption reflects an initial state of the degradation process [18, 19].

3.4 pH

We have determined the change in pH of the aqueous medium as a function of degradation time, thereby testing the liberation of acidic waste from both the PLLA film and scaffold samples, which provides an indication of the state of degradation: greater formation of lactic acid, which is a PLLA degradation product, means greater changes in pH [35, 36]. The liberation of acidic products during the *in vivo* degradation process increased the inflammatory response of the tissue [15].

The changes in pH of both the PLLA and the PLLA/nHA scaffolds and films are shown in Fig. 6a, b as a function of *in vitro* degradation and we see that they all followed a similar behavior up until the fourth week of degradation: pH suffered a slight fall up until the fourth week, and started to recover until it subsequently returned to more or less the

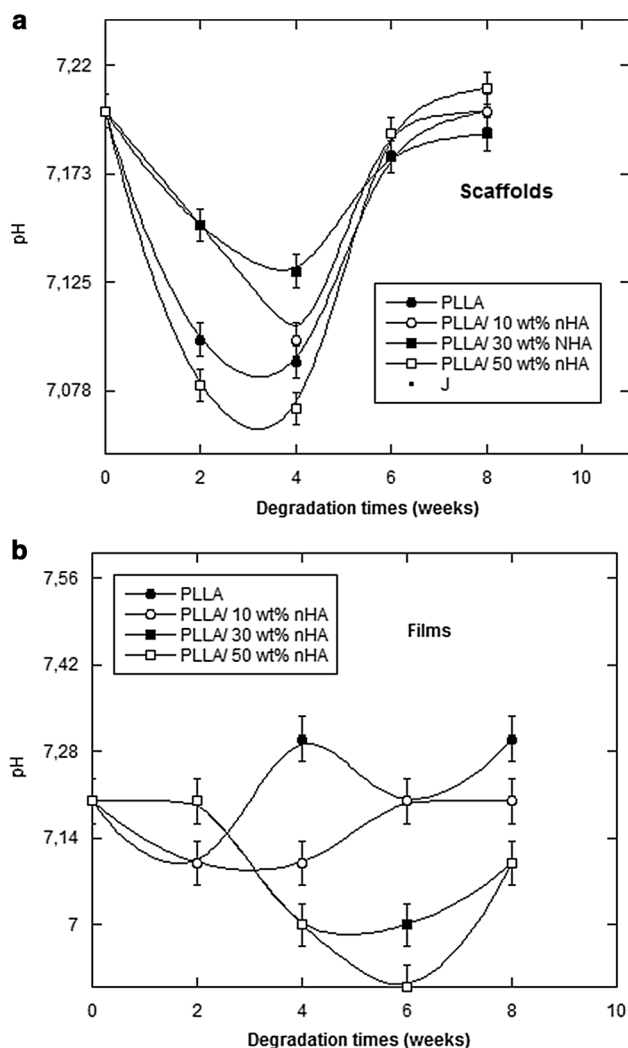


Fig. 6 a pH change of phosphate buffer solution of scaffolds against degradation time (weeks). b pH change of phosphate buffer solution of films against degradation time (weeks)

original value and remained constant up until week 8. The scaffolds were the exception with higher contents of nHA, in which the pH continued with slight increases up until the degradation period under study.

The behavior of the films was completely different (see Fig. 6b), both for the PLLA samples and for the PLLA/nHA 10 wt% samples, the latter sample having less nanohydroxyapatite, in which the pH undergoes a slight fall until the second week of degradation after which it increases over. However, the fall in pH continued in the samples with higher contents of bioactive PLLA/nHA 30 wt% and PLLA/nHA 50 wt% particles until the sixth week of degradation and from the sixth to the eighth week both samples increased their pH. At the end of the eighth week, the sample that had a pH above the initial value was the one with no nHA, reaching a pH of approximately 7.3, and was the most visibly

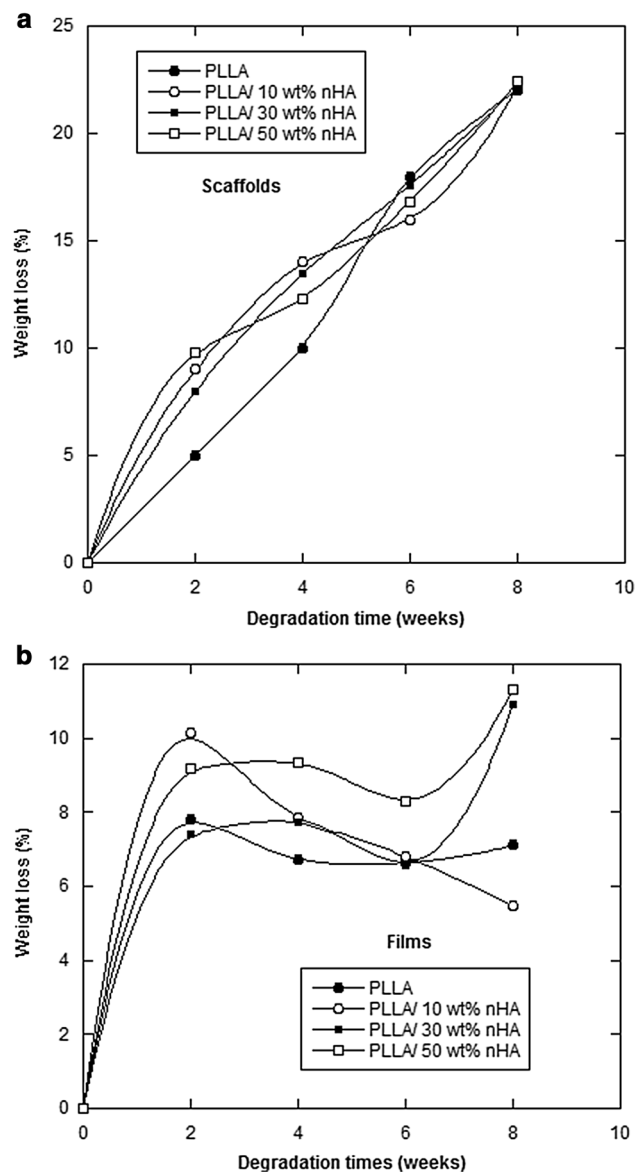


Fig. 7 a Weight loss of scaffolds against degradation time (weeks). b Weight loss of films against degradation time (weeks)

degraded sample. It appears that the nanoparticles acted as a modulator of pH.

3.5 Weight Loss

Usually, degradation rates of the polymer were affected by their structure, molecular weight, and other structural characteristics. Weight loss is an index for the loss of water-soluble oligomers that are formed by hydrolysis and then released from the PLLA into the surrounding media [15].

In Fig. 7a, b, we can see the variations in scaffolds and films weight loss as a function of degradation time; as may be observed, the behavior of both is very different. When

the degradation time increased, the scaffolds underwent an increase in percentage weight loss, although the weight loss for the sample without nHA was not significant until the fourth week of degradation and for the scaffolds with a different composition of nHA, the weight loss started to be considerable in the first week of immersion in PBS at 37 °C. At the end of the degradation process under study, all the samples had undergone weight loss of around 22%.

It was possible to distinguish three stages (Fig. 7b) in the behavior of the films subjected to *in vitro* degradation processes in PBS at 37 °C: a high loss of weight following an almost linear function took place in the first stage; then a second stage from week 2 to week 6 in which a stabilization was noted; followed by a third stage in which a very high loss of weight reoccurred that followed an almost linear function in the samples with a higher content of nHA (30 and 50%) and stabilization for the other samples. In general, we can say that the loss of weight in the samples of higher nHA content was around 11% at the end of the degradation process under study, as against 7% for the samples with 10% of nanoparticles. The introduction of large quantities of nanohydroxyapatite in the films increased the degradation speed.

3.6 SEM

We have studied, the evolution of the *in vitro* degradation process, through Scanning Electronic Microscopy (SEM) for the pure PLLA and PLLA/nHA films and scaffolds. We can see micrographs of PLLA and PLLA/nHA in Figs. 8a and 9. The TIPS technique to manufacture scaffolds is a complex process. Solvent crystallization can induce phase separation when the temperature is lowered to produce a solid–liquid phase separation. When the temperature of the solution is lowered, the solvent crystallizes and the polymer is expelled from the crystallization front of the solvent, so the polymeric solution undergoes a solid–liquid phase separation. The morphology of the crystals of the solvent changes with the type of solvent, the polymer concentration, the temperature of crystallization, and the gradient of temperature applied to the polymeric solution [16].

The scaffolds fabricated in this way are of a very anisotropic tubular morphology with an internal structure that is similar to a stairway. The cavities are parallel to the direction of solidification and have repetitive partitions. The progression of the crystallization front of the solvent defines the principal orientation of the pores, the long parallel axes to the direction of cooling. The diameter of the cavities and the space changes with the speed of cooling, the polymer concentration, and the type of solvent.

The introduction of nanoparticles in the polymeric solution disturbed the crystallization of the dissolvent, changing the process of crystal growth and leaving smaller and more

irregular pores and a more anisotropic structure as the nanoparticle concentrations increased [17].

During the process of *in vitro* degradation (8 weeks), no changes were appreciated in the micrographs that were obtained, only an increase in the porosity of the pore walls over various weeks of degradation. 8 weeks appeared insufficient to obtain significant changes in the degradation of the scaffolds.

In Fig. 9, the films with no degradation and with 0, 10, 30, 50% of nanohydroxyapatite may be seen. As the content of bioactive particles increase in these micrographs, despite dispersion with the sonicator in their manufacturing process, they tend to agglomerate. This behavior is especially observed in the sample with the highest percentage of nHA (50%). Visual observation of the films reveals that they are transparent in the absence of both nHA and water, and they turn even whiter as the content of nanoparticles and water absorption increases. Their surface is irregular and has small rugged zones quite certainly caused by the evaporation of chloroform that causes the polymer to contract. In addition, when in contact with the PBS solution, the films became more fragile and breakable [14, 15].

The effect of the degradation process on films may be seen in Fig. 9, where the first pores appeared as from the second week in PBS, corresponding to the advancing degradation of the samples with 0 and 50% nHA. The films presented high surface porosity and ruggedness from week 6. White products appeared on the samples synthesized with 10 and 30% nHA as the weeks of degradation elapsed, which rather than nanoparticles, were products resulting from the advance of degradation. In addition, we can see that the film that has no nanoparticles was transformed from a whitish color during the *in vitro* degradation process.

The micrographs revealed that the films were degraded before the scaffolds. The scaffolds were stable over the 8 weeks of the degradation process; however, some films lost their integrity after the fourth week of degradation. The films shared a heterogeneous degradation with regard to the surface, with some zones more degraded than others, due to autocatalytic degradation [14, 15].

4 Conclusions

In vitro degradation of PLLA/nHA films and scaffolds composites has been studied. Reinforcement with nHA particles has been shown to increase the modulus of elasticity and yield stress, although the increase was not proportional to the percentage of nanoparticles. The elastic modulus and the yield stress of the films decreased faster than those of the scaffolds. The enthalpy of fusion of the scaffolds was higher than that of the films, which may indicate that crystalline domains are formed more easily in scaffolds. Comparing the

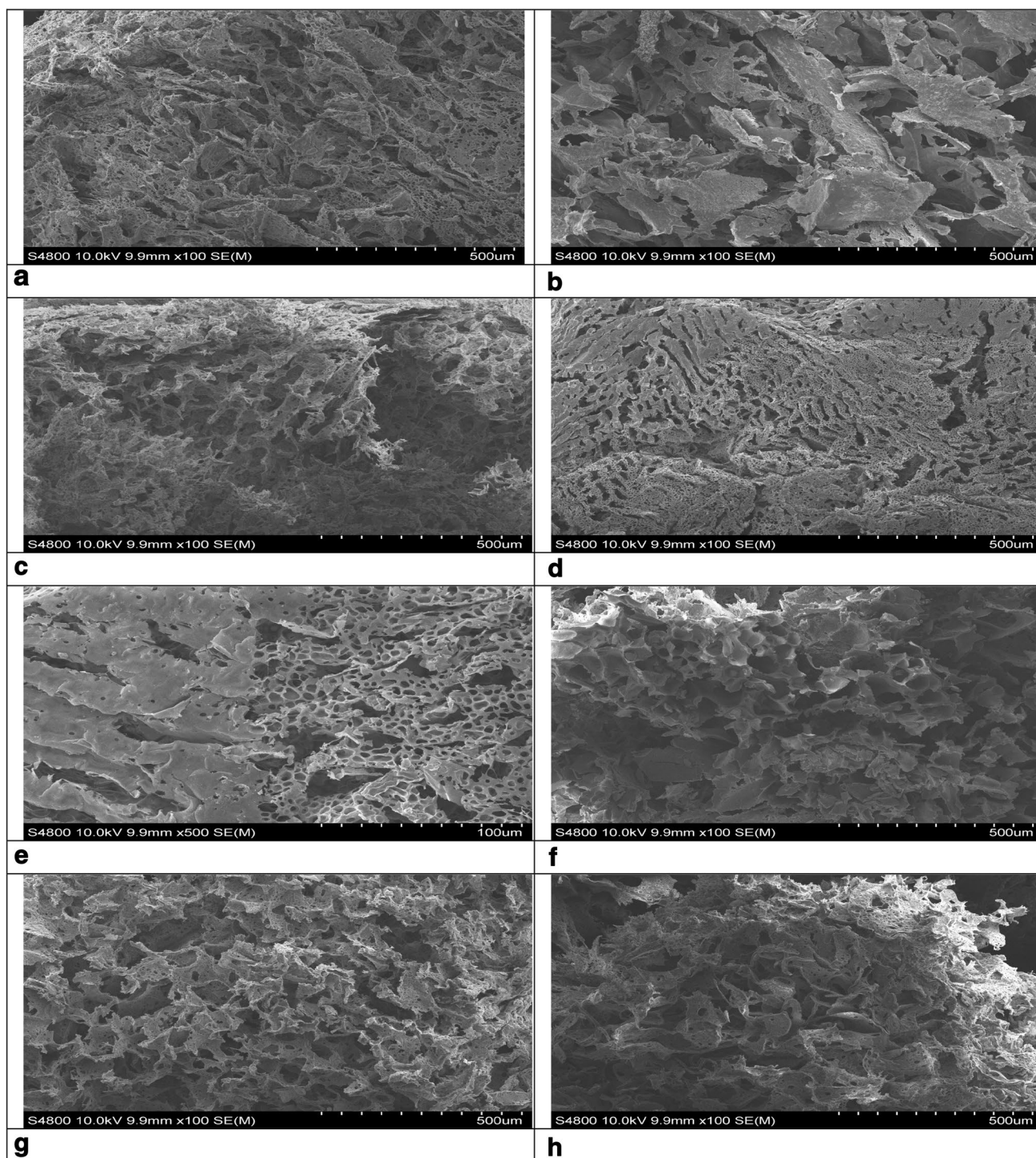


Fig. 8 SEM observation of surface morphology of PLLA scaffolds. **a** PLLA **b** PLLA after in vitro degradation for 8 weeks. **c** PLLA/10 wt% nHA. **d** PLLA/10 wt% nHA after in vitro degradation

for 8 weeks. **e** PLLA/30 wt% nHA. **f** PLLA/30 wt% nHA after in vitro degradation for 8 weeks. **g** PLLA/50 wt% nHA. **h** PLLA/50 wt% nHA after in vitro degradation for 8 weeks

degradation processes for films and scaffolds, we can conclude that the films degraded more rapidly and in a heterogeneous way (there was a difference between some zones or others), due to the acidic products from the degradation process

that are more difficult to evacuate from the films than from the scaffolds and the autocatalytic effects assumes more importance in the films. Likewise, porosity was decisive in the rate of degradation. These results are not extrapolable to

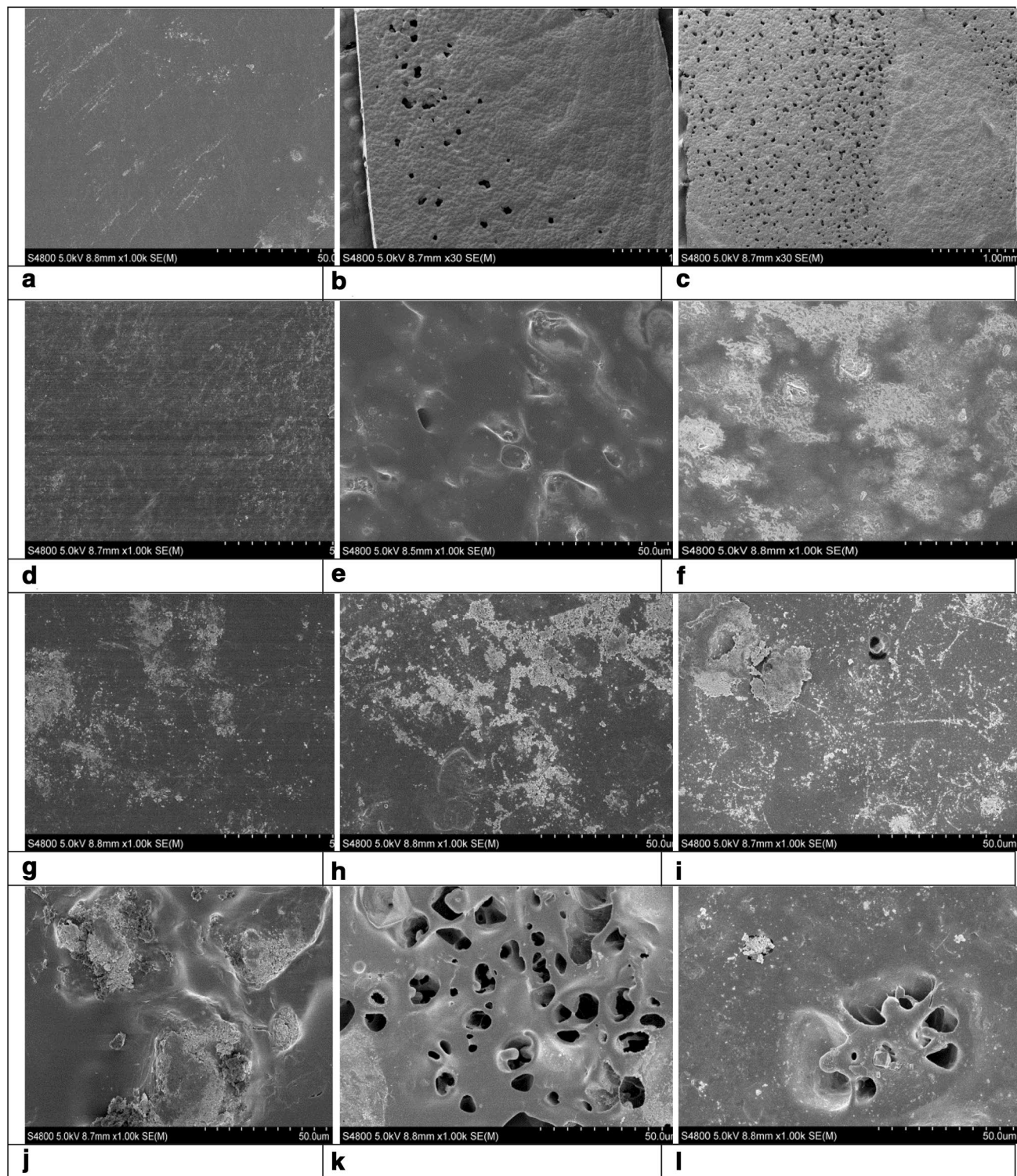


Fig. 9 SEM observation of surface morphology of PLLA films **a** PLLA. **b** PLLA in vitro degradation 6 weeks. **c** PLLA in vitro degradation 8 weeks. **d** PLLA/nHA 10 wt%. **e** PLLA/nHA 10 wt% in vitro degradation 6 weeks. **f** PLLA/nHA 10 wt% in vitro degra-

ation 8 weeks. **g** PLLA/30 wt%. **h** PLLA/30 wt% in vitro degradation 6 weeks. **i** PLLA/30 wt% in vitro degradation 8 weeks. **j** PLLA/50 wt%. **k** PLLA/nHA 50 wt% in vitro degradation 6 weeks. **l** PLLA/nHA 50 wt% in vitro degradation 8 weeks

the in vivo conditions, but they offers valuable information on the behavior of that material in vivo.

Acknowledgements Technical and human support provided by SGIker (UPV/EHU, MICINN, GV/EJ, ERDF, and ESF) are really appreciated.

Author Contributions ALM, IS, IP and ED conceived and designed the experiments; ALM and IS performed the experiments; ALM, IS, IP and ED analyzed the data; ED contributed reagents/materials/analysis tools; ED wrote the paper.

Compliance with Ethical Standards

Conflict of interest The authors declare no conflict of interest.

References

- B.D. Ulery, L.S. Nair, C.T. Laurencin, *J. Polym. Sci. B* **49**(12), 832–864 (2011)
- B. Patel, S. Chakraborty, *J. Excip. Food Chem.* **4**(4), 126–157 (2013)
- H. Patel, M. Bonde, G. Srinivasan, *Trends Biomater. Artif. Organs* **25**(1), 20–29 (2011)
- R.J. Kroeze, M.N. Helder Leon, E. Govaert, T.H. Smit, *Materials* **2**, 833–856 (2009). <https://doi.org/10.3390/ma2030833>
- E. Marin, M.I. Briceño, C. Caballero-George, *Int. J. Nanomed.* **8**, 3071–3091 (2013)
- R.S. Langer, N.A. Peppas, *Biomaterials* **2**, 201 (1981)
- R.S. Langer, L.G. Cima, E. Wintermantel, *Biomaterials* **11**, 738 (1990)
- N.B. Graham, *Chem. Indus.* **15**, 482 (1990)
- K.H. Lam, P. Nieuwenhuis, I. Molenaar, *J. Mater. Sci.: Mater. Med.* **5**(4), 181 (1994)
- J.M. Schakenraad, P. Nieuwenhuis, I. Molenaar, et al. *J. Biomed. Mater. Res.* **23**, 1271 (1989)
- A. Gopferich, *Biomaterials* **17**, 103 (1996)
- F. Burkersroda, L. Schedil, A. Gopferich, *Biomaterials* **23**, 4221 (2002)
- G. Fuentes, Y. Hernández, Y. Campos, *Latin Am. Appl. Res.* **38**, 105 (2008)
- Y. Monhammedi, E. Jabbari, *Macromol. Theory Simul.* **15**, 643 (2006)
- P. Elzbieta, M. Elzbieta, *J. Mater. Sci.: Mater. Med.* **19**, 2063 (2008)
- H. Zeqiang, X. Lizhi, *J. Macromol. Sci. B* **49**, 1069–1082 (2010)
- E. Díaz, I. Puerto, I. Sandonis, I. Ibáñez, *Polymer-plastics technology and engineering. Polym.-Plast. Technol. Eng.* **53**, 150 (2014)
- E. Díaz, I. Puerto, I. Sandonis, I. Ibáñez, *Polym. Eng. Sci.* **54**(11), 2571 (2014)
- Y. Wang, L. Liu, S. Guo, *Polym. Degrad. Stab.* **95**(2), 207–213 (2010)
- Z. Zhou, Q. Yi, L. Liu, X. Liu, Q. Liu, *J. Macromol. Sci. B*, **48**, 309 (2009)
- P. Gentile, V. Chiono, I. Carmagnola et al., *Int. J. Mol. Sci.* **15**, 3640 (2014)
- D.E. Owens, N.A. Peppas, *Int. J. Pharmacol.* **307**(360), 93 (2006)
- R. Zhang, P.X. Ma, *Biodegrad. Compos. Scaffolds* **10**, 446 (1999)
- P.X. Ma, J.W. Choi, *Tissue Eng.* **7**(1), 23 (2001)
- J.S. Bergström, D. Hayman, *Ann. Biomed. Eng.* **44**, 330 (2016)
- S. Farah, D. Anderson, R. Langer, *Adv. Drug Deliv. Rev.* **107**, 367–392 (2016)
- D. Rasselet, A. Ruellan, A. Guinaultet, al., *Eur. Polym. J.* **50**, 109 (2014)
- R. Pantani, A. Sorrentino, *Polym. Degrad. Stab.* **98**, 1089 (2013)
- M.J. Richardson, in *Comprehensive polymer science*, ed. by C. Booth, C. Price (Pergamon, Oxford, 1989), p. 867
- S.M. Li, H. Garreau, M. Vert, *J. Mater. Sci.* **1**, 131 (1990)
- J.W. Leenslang, A.J. Pennings, R.R. Bos, *Biomaterials* **8**, 311 (1987)
- C. Plummer, C.J. Bourban, P.E. Manson, *J. Mater. Sci.-Mater. Med.* **23**, 1371 (2012)
- C. Efe, F. Ozaydin, H. Ucisik et al., *Therm. Anal. Calorim.* **125**, 659 (2016)
- J. An, C.K. Chua, K.F. Leong, C.H. Chen, J.P. Chen, *Biomed. Microdev.* **14**(5), 863–872 (2012)
- S. Naznin, H.K. Tareef, *J. Nanomater.* (2013). <https://doi.org/10.1155/2013/479109>
- E. Vey, C. Roger, L. Meehan, J. Booth, M. Claybourn, A.F. Miller, A. Saiani, *Polym. Degrad. Stab.* **93**, 1869 (2008)